IN SITU CONSIDERATION OF RESISTANCE OF BRIDGE GIRDER ACCORDING TO EC2 WITH AEM

Ana Brunčič[1,*], Andrej Štrukelj[2], Maja Kreslin[1], Andrej Anžlin[1] and Aljoša Šajna[1]

[1]Slovenian National Building and Civil Engineering Institute;
ana.bruncic@zag.si, maja.kreslin@zag.si, andrej.anzlin@zag.si, aljosa.sajna@zag.si
[2]University of Maribor, Faculty of Civil Engineering, Transportation Engineering and Architecture;
andrej.strukelj@um.si
*Correspondence: ana.bruncic@zag.si

ABSTRACT

The paper presents a case study of a considerably cracked and degraded bridge in Slovenia: with the implementation of in-situ measurements under bending and shear and the use of a non-destructive acoustic emission technique. Despite the existing crack system, the latter was able to detect microstructural changes. These were characterised by low values of average frequency (AF), as well as lower values of the rise time-amplitude ratio (RA), and energy. A correlation between shear capacity and acoustic activity was observed. This promises to expand the use of AE in the process of assessing of the load-bearing capacity of existing concrete structures.

Keywords: Shear resistance, shear crack, crack width, acoustic emission (AE) parameters, bridge girder, stiffness, elasticity, damage evaluation.

1. Introduction

The acoustic emission (AE) technique is provenly one of the non-destructive techniques (NDT) sensitive to damage initiation and progress in reinforced concrete (RC) structures. It can detect the onset of failure and identify its mode more accurately than any other NDT [1-3]. Shear deformations obtain AE events with longer waveforms and lower frequencies, while volumetric changes of material significant for tensile AE events are recognisable for their shorter duration and higher frequencies [1, 2], [4]. The first type of fracture in the material is known as mode II of cracking and the second one as mode I, since mode I is significant for the first stages of fracture during crack opening and mode II for the progression of fracture causing fretting or sliding [5]. Besides the number of counts and energy released, rise time (RT), defined as the delay between the onset and the highest waveform peak, and the RA value, giving the ratio of RT to maximum amplitude (A), appeared to be the most sensitive to the stress field changes in material [2, 3], [6-8]. Due to its passive nature, AE technique was already noticed as an application giving useful qualitative and quantitative insight into structural response when performing bridge health monitoring even under live load conditions [3, 4]. However, the vast majority of the tests were performed in the laboratory, mostly with cyclic loading and un-loading test protocols [5, 9].

Several effects were observed while tracking damage progression in material under loads, such as Kaiser effect or Felicity effect. The first one, naming phenomena when material emits acoustic waves only after a primary load level is exceeded, has been shown to exist at 70 to 85 % of ultimate strength in concrete material. The latter, describing the absence of the Kaiser effect, is more

significant for composite material [4]. Quantification of obtained AE data is mostly done with statistical analysis, preferably given through Historic and Severity indices [4] or b-value [8].

In the last decades, the structural safety of the existing infrastructure has become an important issue in Europe [10]. The reliability of the bridges is of special concern due to their indispensable role in transport connections, increase of the expected traffic load and degradation of a material due to environmental actions [10, 11]. Slovenian bridges built in the second half of the twentieth century are of particular concern due to their structural system, substandard shear reinforcement, negligible concrete cover and insufficient maintenance. Deterioration of concrete and corrosion of the reinforcement are the main damage mechanisms leading to the decrease of load-bearing capacity. This is hardly determinable by visual inspection despite evident deflections and cracks. Accurate evaluation of load bearing capacity, especially shear resistance, is thus rather difficult without drastic interventions in the structure of the bridge.

To obtain more information on the shear resistance of existing bridges with existing shear cracks case study of *in-situ* test was executed with a controlled loading condition on an approx. 60 years old two-span reinforced concrete (RC) bridge. It was assessed as unsafe for use and scheduled for replacement. The structural response of the bridge was monitored continuously through measurements of crack width, deflection, and collection of AE data. The structural performance of the bridge was analysed with the finite element method (FEM) based on the theory of elasticity and shear resistance evaluated by the criteria given in EN 1992-1-1 [12]. In this case study only edge girder of the bridge deck, with shear crack 0.9 mm wide was analysed.

2.   Case study of a girder reinforced concrete bridge

2.1 Bridge structure and material properties

This two-span girder bridge was located in Slovene village, ensuring passage of local road over river. No data exist about the bridge design, construction, or maintenance. The superstructure of the bridge was comprised of two spans, each long 14.0 m, as shown in Fig. 1. Series of five girders assembling the deck of each span, as seen in Fig. 1, was bound together with transversal cross beams as shown in Fig. 3, and deck slab, giving significant rise of stiffness of the girder system. The railing of the bridge was removed before the test. Material properties were rather estimated than determined. Compressive strength f_c of concrete was assessed to be approx. 25 MPa – obtained indirectly through rebound number obtained with Proceq Original Schmidt hammer OS8000 without any core drilled and destructive compression tests performed. Modulus of elasticity of concrete E_c was assessed on several girders with ultrasonic pulse velocity tester Pundit 200. The average value of 23.6 GPa and Poissons number 0.30 were therefore assumed in FEM analysis. Other material properties of concrete were adapted by Eurocode 2 (EC2) [12]. Material properties of steel were attributed to tests performed on other similar bridges with embedded smooth steel reinforcement: yielding strength was assigned to be 250 MPa, strain at maximal stress ε_{su} 10 %, and modulus of elasticity E_s 190 GPa. All material properties are listed in Table 1, with the designation used in EC2. Distribution and size of steel reinforcement were determined using Proceq profoscope and verified with destructive testing: ending girders were assessed to have embedded 8 bars of 28 mm diameter placed in 2 rows as longitudinal reinforcement (Fig. 3) and stirrups of 10 mm diameter placed on average distance of 40 cm as shear reinforcement (Fig. 4). Condition state of the bridge is shown in Fig. 2.

According to estimated material and geometry properties bending capacity M_{ult} of edge girder was determined to be 1100.4 kNm with failure of concrete in compression ($\varepsilon_c/\varepsilon_s$ = 3.5 ‰/10.2 ‰), moment at which yielding of reinforcement occurs M_{rf} 1048 kNm, and cracking moment M_{cr} was calculated to be 148.6 kNm. Shear resistance was determined following Eurocode 2 [12], namely as shear resistance of concrete with included dowel action and aggregate interlock V_c 155.2 kN, shear resistance of concrete with stirrups by generalised stress field approach V_{sw} 97.7 kN with limiting the capacity of diagonal strut V_{max} 1446.2 kN.
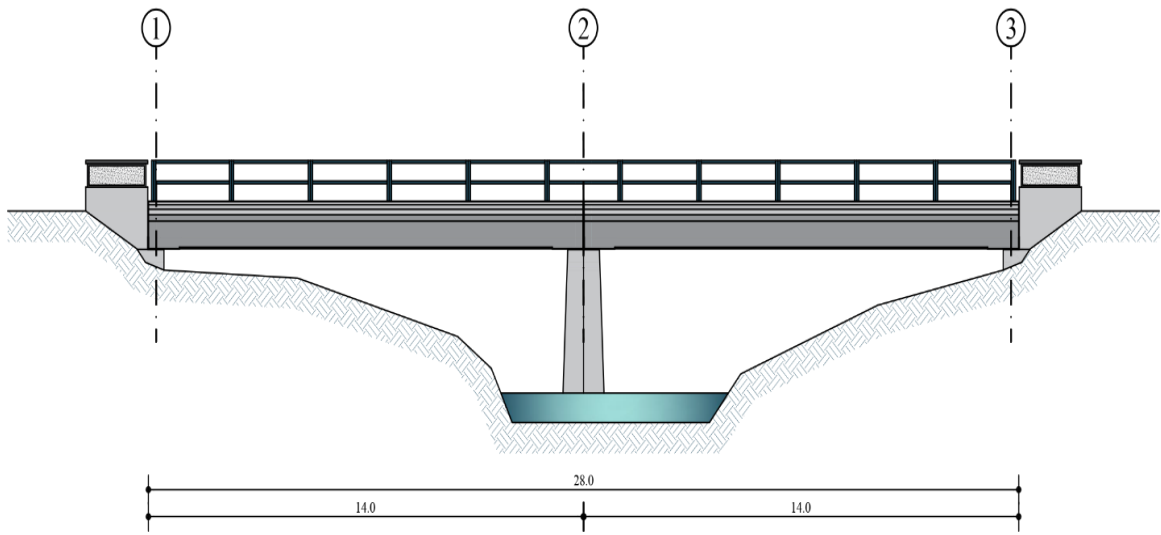
Fig. 1: Side view of a two-span girder bridge.

Fig. 2: Location of bridge (upper left), abutment with bearing of end girder (upper right), deterioration of concrete and steel corrosion (down left), shear cracks 0.9 m wide (down right).
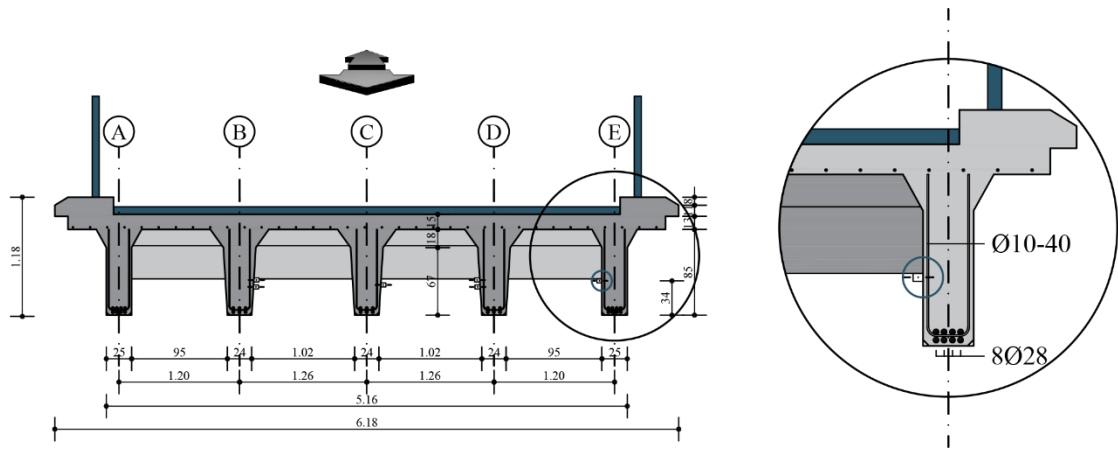
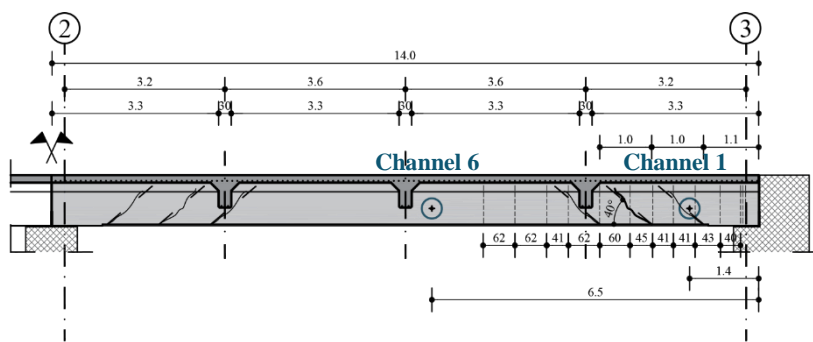Fig. 3: Cross-section geometry of the two-span girder bridge.

Fig. 4: Tested bridge span with indicated cross beams distributed over the length of girder system, positions of AE sensors (circles with dots), monitored shear crack (at a distance 2.1 m from the right end of girder) and indicated distribution of stirrups.

Table 1: Mechanical properties of concrete and steel.

CONCRETE		STEEL	
f_c (MPa)	25	f_y (MPa)	250
ε_{c3} (‰)	1.75	ε_y (‰)	2.0
ε_{cu3} (‰)	3.5	ε_u (%)	10.0
E_c (GPa)	23.6	E_s (GPa)	190

2.2 Test loading protocol

The loading was carried out with two types of concrete blocks, weighing approx. 2.5 t and 1.1 t. Each concrete block was weighed while being placed on the bridge deck by the crane. Two types of loading were performed successively: 1) a *three-point bending test* with the concentration of the concrete blocks in the mid-region of the span and 2) a combination of *shear and bending test* with the shift of half of the concrete blocks already placed at the midspan to the left of the most pronounced shear crack on egde girder. Both tests were performed successively: one after another without un-loading phase.

The loading history of both performed tests with the cumulative weight of concrete and the weight of each concrete block is shown in Fig. 5.
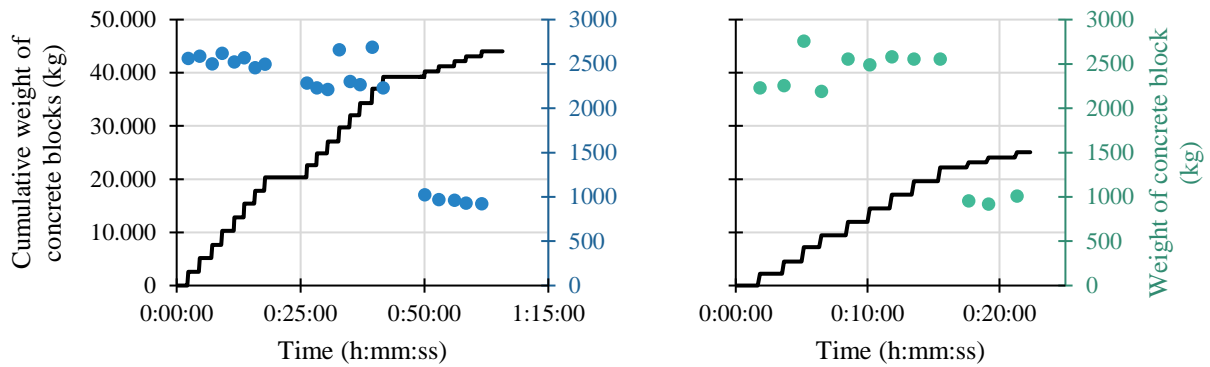
Fig. 5: Loading history of three-point bending test (left) and shear test (right).

2.3 Measured quantities and equipment setup

In order to assess the resistance of the structure and its behaviour, three types of data were acquired: 1) load weight, 2) deformations of structure (deflections and crack width) and 3) AE signals and their properties.

Load weight was measured with the weighting sensor RSCC3/5T-1 of capacity 5 t from Hottinger Baldwin Messtechnik (HBM). Measurements were performed on the crane arm during the lifting and placement of concrete blocks.

Mid-span displacement was measured on the upper side of both curbs and at the bottom of the middle girder with HBM's inductive displacement transducers (IDT) of type WA/100 mm. Crack width was measured on the inner side of the end girder on the downstream side with the self-made sensor. All measurements of deformations were computer controlled and processed with HBM's CATMAN-AP software.

The AE data acquisition was carried out with an outdoor DiSP-workstation unit. Real-time monitoring was enabled by the AEWin software and the acquisition system. Prior to acquiring any actual load test data, pencil lead break (PLB) tests were performed close to all sensors to check their sensitivity. Two sensors were placed on the end girder where crack width and displacement were measured, both approx. at the middle of web. First one was placed 1.4 m from end of the beam in the vicinity of the observed crack (Channel 1), and the second one 6.5 m from the end, near mid-span (Channel 6) as seen from Fig. 4. Threshold level was set to 45 kHz. All measurements and acquisitions were synchronised.

2.4 Structural analysis

To evaluate and compare the resistance of girder under observation, structural analysis with finite element method (FEM) was performed, based on obtained data. The system of longitudinal girders and transversal stringers was modelled with beam elements, with a T-shaped cross-section, and a deck slab with plate elements, as seen from Fig. 6. Maximal element size was 20 cm. Measured displacements indicated partial clamping at the middle and end support which was determined upon iteration during calibration of displacements. With the addition of bending stiffness at support 2 (Fig. 2) was 2×10^4 kNm/rad and 10^3 kNm/rad at support 3 roller supports was changed to partially clamped support. Loads were applied as surface load areas, contributed according to test loading protocol. Software SOFISTIK$^®$ was used for analysis.
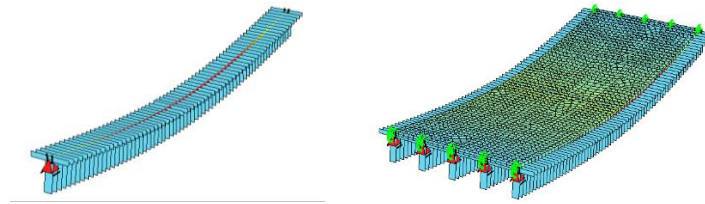
Fig. 6: Model for finite element analysis (girder modelled with beam elements and T cross section – left; deck modelled with plate elements, connected with beam elements in their centre of gravity).

3. Results

Obtained data from displacement measurements indicate linear elastic behaviour of structure during bending tests (Fig. 7) with ratio u_{el}/u 1.0. Soon after the beginning of the shear-bending test, elasticity theory could not be applied anymore since the ratio u_{el}/u dropped to approx. 0.5 with the apparent loss of initial stiffness, still it was used for determination of the load amount.
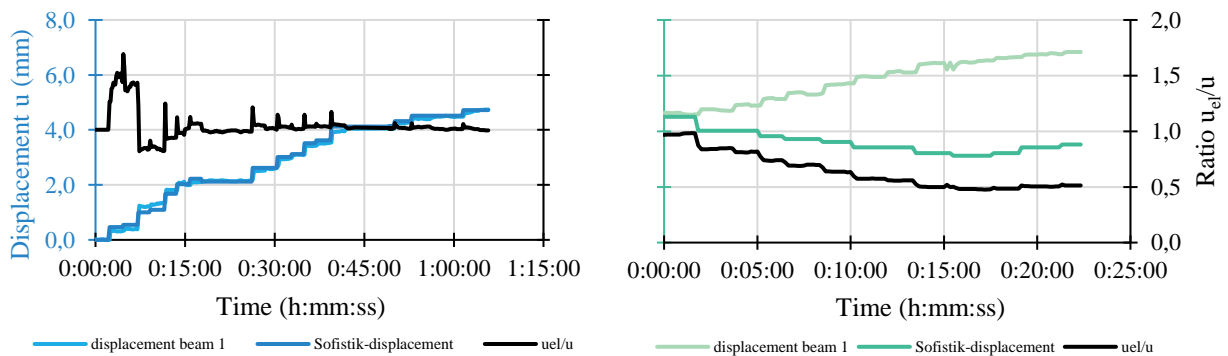

Fig. 7: Comparison of measured and calculated displacements: bending test (left) and shear test (right).

Correlation between crack width and displacement was retained throughout both tests with a notable difference in the behaviour of superstructure (Fig. 10): more pronounced increment of displacement of mid-span in bending test (blue) and crack width in shear test (green).
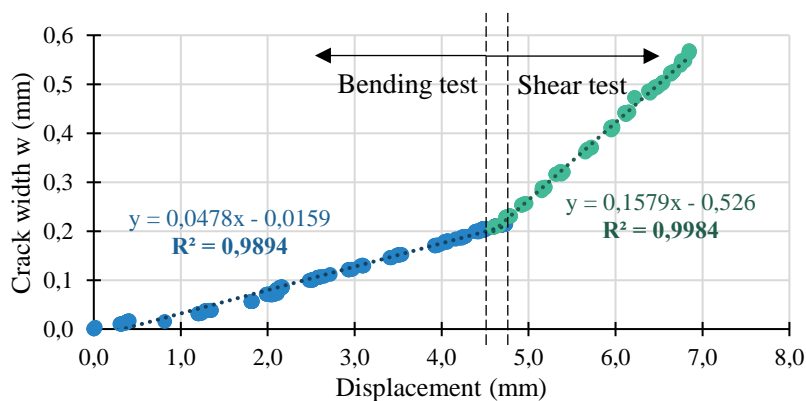

Fig. 8: Correlation between the measured displacement and crack width.

The time-dependent values of some typical AE parameters are depicted in Fig. 9 and 10. The line is the moving average of 20 counts.
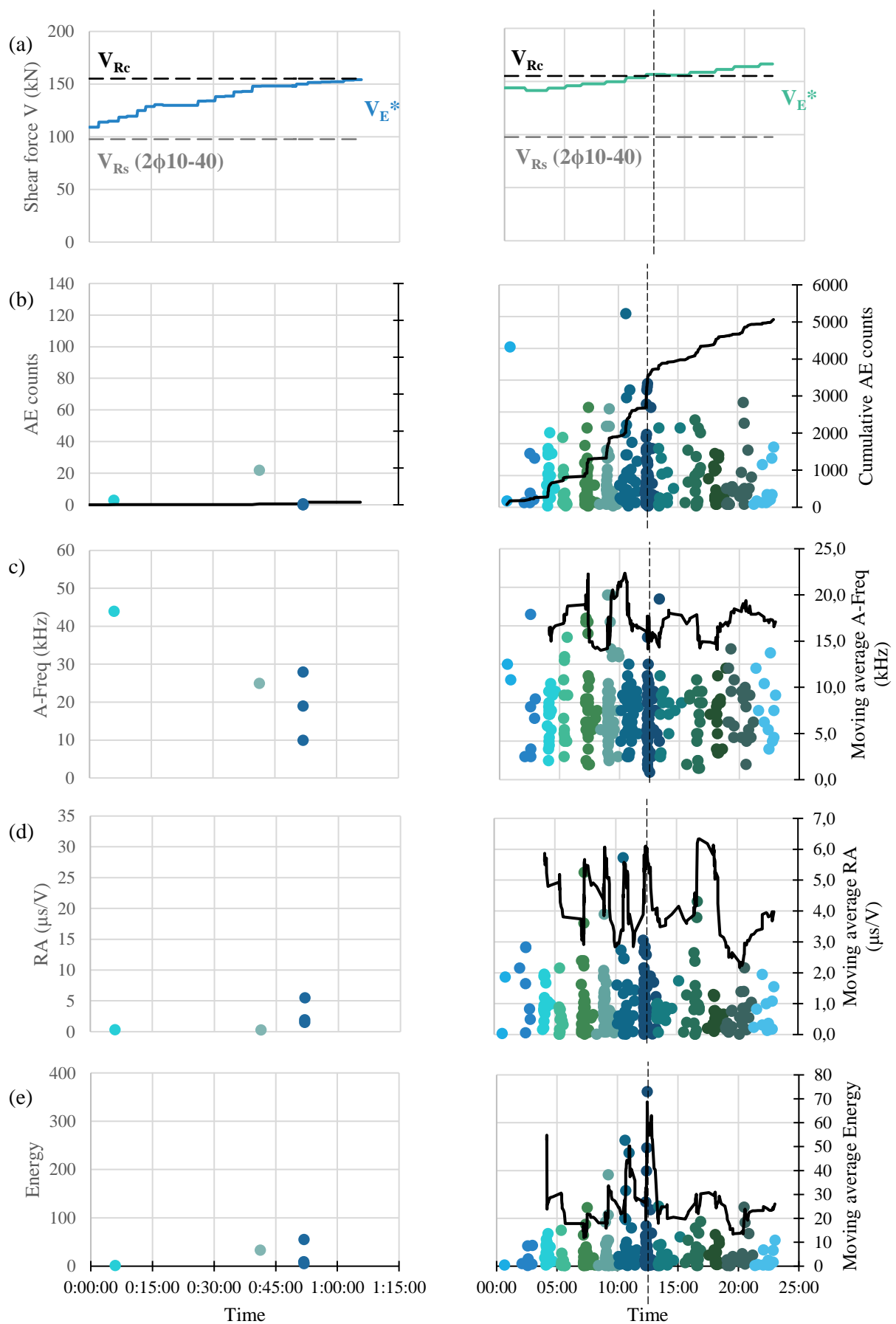
Fig. 9: Time history of (b) accumulated AE activity, (c) Average frequency, (d) RA, and (e) AE energy for the three-point bending test (left) and shear test (right) with shear force diagram (a) for Channel 1.
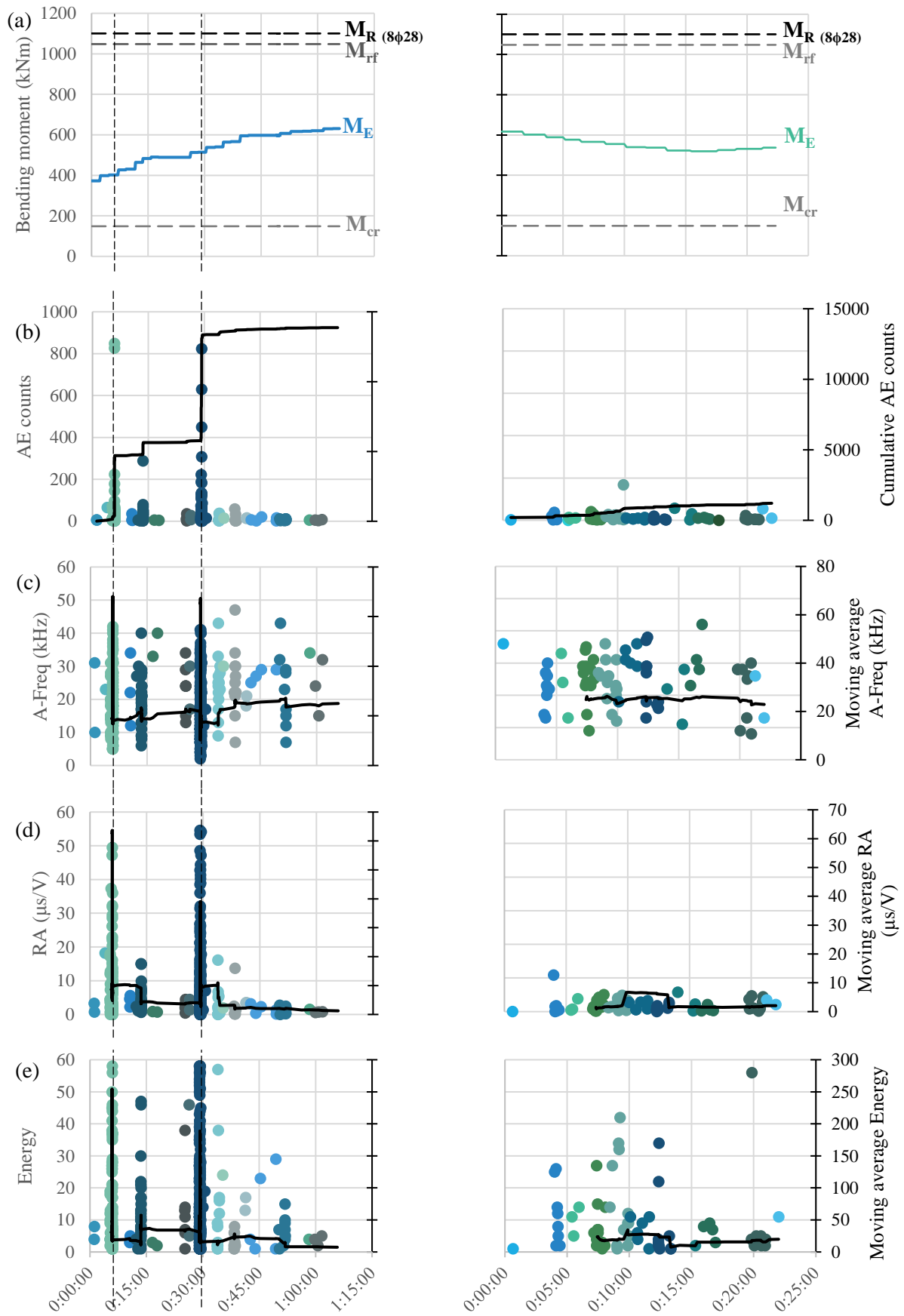
Fig. 10: Time history of (b) accumulated AE activity, (c) Average frequency, (d) RA, and (e) AE energy for the three-point bending test (left) and shear test (right) with shear force diagram (a) for Channel 6.
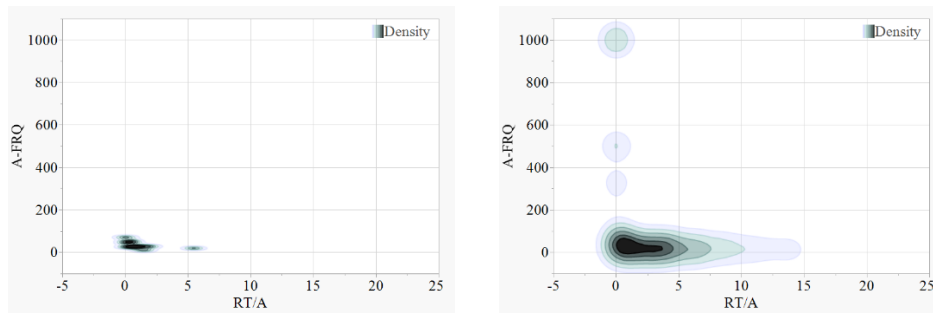
Fig. 11: Density scatter plot of AF/RA values of Channel 1 (left – three point bending test; right – shear test).
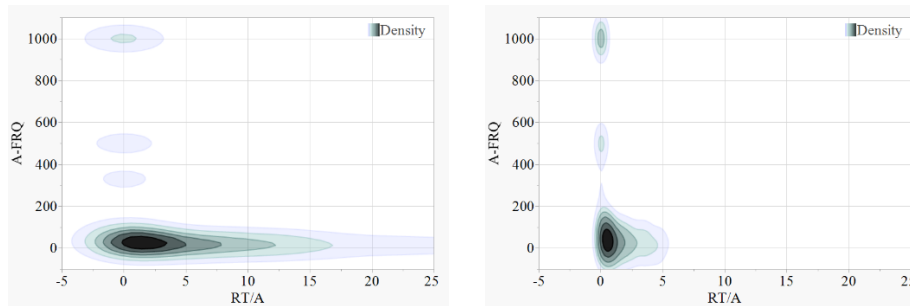

Fig. 12: Density scatter plot of AF/RA values of Channel 6 (left – three point bending test; right – shear test).

Slightly increased AE activity can be noticed in the mid-span of the girder during the bending test (Fig. 9 and 10): two peaks of AF, RA, and energy show weak intensification of micro cracking still, average values remain quite low and cannot be associated with the presence of any live and active cracks. As seen in Fig. 12 type of deformation was mostly intergranular and transgranular. Regarding bending resistance of girder, no major fracture mechanisms were expected, since load applied was not in range of yielding of longitudinal reinforcement or rupture of girder. General AE activity was lower in the shear test (Fig. 9 and 10), the number of recorded hits is almost three times smaller than the number of hits accumulated in the bending test. As in the bending test, average values of AF, RA and energy are low. However, they still demonstrate a connection with the resistance of the structure: in the eighth loading step, there is a noticeable increase in AE events, followed by a more quiescent phase with a noticeable drop of energy, AF, and RA values. As in the case of the bending test and seen from Fig. 11 type of deformation was mostly intergranular and transgranular, leading into obvious loss of stiffness and resistance. The coincidence of concrete shear capacity and acoustic activity is apparent, still, it must be noted that elasticity theory and the shear force determined by it cannot be directly applied in the case of performed shear test. Since, with any of the tests, the ultimate bearing capacity of the structure was not exceeded, the Kaiser and Felicity effects are not negligible in the interpretation of results. Given the clear pattern of the formed cracks, the question is how much energy can still be released when loading a structure with an unknown loading history.

4. Conclusions

AE is already recognised and established as a useful non-destructive technique for the assessment of microstructural changes in structures of the built environment. Yet examples of the use of AE in the characterisation of micro- and macrostructural changes and consequences leading to the specifics of the structural behaviour of existing structures are rare. From obtained and analysed data we can conclude:

- AE is a method that can give meaningful results even when determining the load capacity of existing structures.
- In the case of decaying structures with significant material degradation and an existing crack system, qualitative analysis can be made with AE, which provides an insight into the condition of the material(s) of the structure and the fracture behaviour of the structure.
- AE values acquired are markedly reduced in case of preexisting cracks, especially values of AF, RA, and energy. However, there are qualitative differences between the data, which enable the identification of additional fractures in the material structure.

The performed data analysis shows the potential of AE. Due to the corrosion of the reinforcement and the questionable adhesion with concrete, more comparative studies of this kind on real objects are needed.

5. Acknowledgments

6. References

[1] D. G. Aggelis, "Classification of cracking mode in concrete by acoustic emission parameters," *Mech. Res. Commun.*, vol. 38, no. 3, pp. 153–157, 2011, doi: 10.1016/j.mechrescom.2011.03.007.

[2] A. C. Mpalaskas, T. E. Matikas, D. G. Aggelis, and N. Alver, "Acoustic emission for evaluating the reinforcement effectiveness in steel fiber reinforced concrete," *Appl. Sci.*, vol. 11, no. 9, 2021, doi: 10.3390/app11093850.

[3] S. Kashif Ur Rehman, Z. Ibrahim, S. A. Memon, and M. Jameel, "Nondestructive test methods for concrete bridges: A review," *Constr. Build. Mater.*, vol. 107, pp. 58–86, 2016, doi: 10.1016/j.conbuildmat.2015.12.011.

[4] A. Nair and C. S. Cai, "Acoustic emission monitoring of bridges: Review and case studies," *Eng. Struct.*, vol. 32, no. 6, pp. 1704–1714, 2010, doi: 10.1016/j.engstruct.2010.02.020.

[5] C. U. Grosse and M. Ohtsu, Eds., *Acoustic Emission Testing*. Springer-Verlag Berlin Heidelberg, 2008.

[6] K. Du, X. Li, M. Tao, and S. Wang, "Experimental study on acoustic emission (AE) characteristics and crack classification during rock fracture in several basic lab tests," *Int. J. Rock Mech. Min. Sci.*, vol. 133, no. August 2019, p. 104411, 2020, doi: 10.1016/j.ijrmms.2020.104411.

[7] V. N. Nerella, M. Nather, A. Iqbal, M. Butler, and V. Mechtcherine, "Inline quatification of extrudability of cementitious materials for digital construction," *Cem. Concr. Compos.*, no. 95, pp. 260–270, 2019.

[8] D. D. Mandal *et al.*, "Acoustic Emission Monitoring of Progressive Damage of Reinforced Concrete T-Beams under Four-Point Bending," *Materials (Basel).*, vol. 15, no. 10, p. 3486, 2022, doi: 10.3390/ma15103486.

[9] M. Ohtsu, "Acoustic Emission (AE) and Related Evaluation (NDE) Techniques in the Fracture Mechanics of Concrete," no. 2nd Edition, p. 330, 2020.

[10] Y. Yang, D. A. Hordijk, and A. De Boer, "Acoustic emission study on 50 years old reinforced concrete beams under bending and shear tests," no. December, 2016.

[11] E. J. Obrien, B. Heitner, G. Causse, and T. Yalamas, "Validation of bridge health monitoring system using temperature as a proxy for damage," no. August 2019, pp. 1–14, 2020, doi: 10.1002/stc.2588.

[12] *EN 1992-1-1 Eurocode 2: Design of concrete structures - Part 1-1: General rules and rules for buildings.* 2004.